Int. J. Electrochem. Sci., 7 **(2012)** 2403 - 2415

International Journal of
ELECTROCHEMICAL
SCIENCE
www.electrochemsci.org

Investigation of Benzimidazole Compound as a Novel Corrosion Inhibitor for Mild Steel in Hydrochloric Acid Solution

Xiumei Wang[*], *Ye Wan, You Zeng, Yaxin Gu*

School of Materials Science and Engineering, Shenyang Jianzhu University, Shenyang 110168, China
[*]E-mail: xmwang@alum.imr.ac.cn

Received: 30 November 2011 / *Accepted:* 21 December 2011 / *Published:* 1 March 2012

The inhibition ability of 1, 4-bis-benzimidazolyl-butane (BBB) on mild steel in 0.5 M HCl solution was studied by weight loss measurements, electrochemical techniques and atomic force microscopy (AFM). BBB inhibited mild steel corrosion in 0.5 M HCl solution significantly and the inhibition efficiency increased with BBB concentration. Potentiodynamic polarization results showed that BBB was a mixed-type inhibitor. The adsorption of BBB on mild steel surface was strong chemical adsorption and followed Langmuir adsorption isotherm. Quantum chemical calculation was further applied to reveal the adsorption structure and explain the experimental results. The inhibition performance of BBB was also evidenced by AFM images.

Keywords: Mild Steel; Polarization; EIS; AFM; Acid Corrosion

1. INTRODUCTION

Organic compounds containing heteroatom such as oxygen, nitrogen, sulphur, phosphorus, multiple bonds, aromatic rings and conjugated π bonds as corrosion inhibitor of mild steel have been paid more and more attention. They have long been used in acid pickling, industrial acid cleaning, acidification of oil wells, acid de-scaling to control acidic corrosion of metals [1-3]. The lone pair electrons of the heteroatom and conjugated bonds can form chemisorptive film on metal surface through interaction with metal surface atoms thus to retard the metal from the corrosion media and create good inhibition effect. Generally, a strong coordination bond causes higher inhibition efficiency, the inhibition increases in the sequence O < N < S < P [4-5]. The efficiency of an organic compound as a corrosion inhibitor depends not only on the characteristics of the environment in which it acts, the

nature of the metal surface and electrochemical potential at the interface, but also on the structure of the inhibitor itself, which includes the number of adsorption active centre in the molecule, their charge density, the molecule size, the mode of adsorption, the formation of metallic complexes and the projected area of the inhibitor on the metallic surface[6-14].

Non-toxic benzimidazole and its derivatives have been proved excellent inhibitors for mild steel [15-17]. Bis-benzimidazole molecule has large size and shows two anchoring sites suitable for surface bonding: the nitrogen atom with its lonely sp2 electron pair and the aromatic rings. Planar benzimidazole ring displays large projected area on metal surface and will show good inhibition effect. The aim of this work is to study the inhibition effect of bis-benzimidazole BBB as a corrosion inhibitor for mild steel in 0.5 M HCl solution by weight loss tests, electrochemical measurements, as well as atomic force microscopy (AFM) studies.

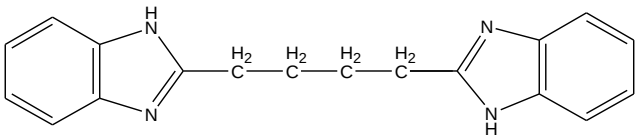

2. EXPERIMENTAL

2.1 Weight loss experiments

Weight loss experiments were carried out on mild steel sheets with wt% composition as follows: C, 0.15; Mn, 0.32; P, 0.05; balance, Fe and with the size of 2 cm × 2 cm × 0.5 cm. The mild steel specimens were abraded by SiC paper successively to grade 800. Then cleaned with bi-distilled water and decreased with acetone and then dried. The bis-benzimidazole compound (1, 4-bis-benzimidazolyl-butane) was shown as follows:

All chemicals and reagents were AP grade and used as source without further purification. The corrosion media were 0.5 M HCl solutions without and with addition of BBB. Tests were performed under static condition in 250 mL solutions at 303 K for 5 h in triplicate. After immersion, mild steel specimens were rinsed with bi-distilled water and cleaned with alcohol-cotton to remove corrosion products. At last, the specimens were weathered, stored in a vaccum drying chamber for 24 h and then weighed. Weight loss allowed us to calculate the mean corrosion rate as expressed in mg cm^{-2} h^{-1}.

2.2 Electrochemical Techniques

A conventional electrochemical cell capacity 250 mL was employed containing three compartments for working, counter and reference electrodes. The working electrode was made of mild steel specimen grinded with emery paper up to 800 grade with the exposed surface area was 0.785 cm^2

and the remainder was embedded with epoxy. The counter electrode and the reference electrode were platinum electrode and saturated calomel electrode (SCE), respectively.

Electrochemical measurements were conducted on a Parstat 2273 system. All the potential are reported referred to SCE. The potentiodynamic polarization curves were obtained at a scan rate of 0.5 mV /s starting from –150 mV to +350 mV (SCE). The electrochemical impedance spectroscopy experiments were obtained in the frequency range of 100 kHz -10 mHz at open circuit potential with amplitude 10 mV peak to peak. Before measurements the working electrode was immersed in the test solution at open circuit potential for 0.5 h until a steady state reached.

2.3 Morphology of the mild steel surface

The morphologies of the mild steel surface in 0.5 M HCl without and with addition of BBB were tested after immersion for 5 h using an atomic force microscopy (AFM) with the mode of Pico Plus 2500.

2.4 Quantum chemical study

The molecular structures of BBB have been fully geometric optimize by PM_3 method with Hyperchem 7.5.

3. RESULTS AND DISCUSSIONS

3.1 Weight loss measurements

The corrosion rate of mild steel with the addition of BBB in 0.5 M HCl solution and inhibition efficiency were listed in table 1. The surface coverage (θ) and inhibition efficiency (*IE* %) were estimated from the following equation [18-19].

$$\theta = \frac{r^0 - r_{\text{inh}}}{r^0} \quad (1)$$

$$IE\% = \frac{r^0 - r_{\text{inh}}}{r^0} \times 100 \quad (2)$$

where r^0 and r_{inh} are the corrosion rates of mild steel in 0.5 M HCl solution without and with addition of BBB, respectively. The corrosion rate of mild steel in 0.5 M HCl solution is greatly reduced upon the addition of BBB. This behavior reflects the inhibition effect of BBB against the mild

steel corrosion in acid solution. And the corrosion inhibition enhances with BBB concentration increasing. This result is the fact that the adsorption amount and the coverage of inhibitor on mild steel surface increases with the increase of BBB concentration.

Table 1. Corrosion rate of mild steel and inhibition efficiency for various concentrations of BBB in 0.5 M HCl solution obtained from weight loss measurements.

C_{inh}	r	IE	θ
/M	/mg cm^{-2} h^{-1}	/%	
Blank	0.3224	-	-
1.7×10^{-5}	0.0784	75.7	0.76
1.0×10^{-4}	0.0636	82.2	0.82
2.0×10^{-4}	0.0432	86.6	0.87
4.1×10^{-4}	0.0393	87.8	0.88
6.8×10^{-4}	0.0386	88.0	0.88

3.2 Potentiodynamic polarization curves

Fig.1 shows that potentiodynamic polarization curves of mild steel in 0.5 M HCl solution without and with addition of different concentration of BBB. The presence of BBB caused a clear decrease in both anodic and cathodic current densities with the increase of BBB concentration, probably due to the adsorption of BBB at the active sites of the electrode surface, retarding both metallic dissolution and hydrogen evolution reactions, and consequently slowing the corrosion processes.

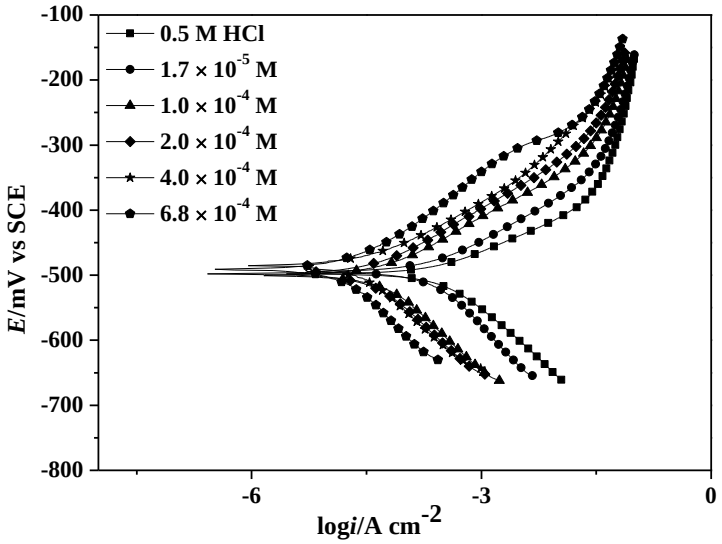

Figure 1. Potentiodynamic polarization curves for mild steel in 0.5 M HCl solution without and with different concentrations of BBB.

The associated corrosion electrochemical parameters, i.e., corrosion potential (E_{corr}), corrosion current density (i_{corr}), cathodic Tafel slope (β_c), anodic Tafel slope (β_a) derived from these curves by extrapolation, as well as the percentage inhibition efficiency (*IE*%) are listed in Table 2. Here, the *IE*% is defined by the following equation [20]:

$$IE\% = \frac{i^0_{corr} - i_{corr}}{i^0_{corr}} \times 100 \quad (3)$$

where i^0_{corr} and i_{corr} are the corrosion current density values without and with BBB, respectively. The results also show that by increasing BBB concentration, the corrosion current density decreased and inhibition efficiency (*IE* %) increased. It can be also observed the corrosion potential values keep almost constant in presence of BBB, suggesting that BBB behaves as a mixed-type inhibitor. Moreover, BBB causes no obvious change in the anodic and cathodic Tafel slope, indicating BBB is first adsorbed onto mild steel surface and therefore impedes by only blocking the reaction sites of mild steel surface without affecting the anodic and cathodic reaction mechanism [21].

Table 2. Electrochemical parameters obtained from potentiodynamic polarization curves measurements of mild steel in 0.5 M HCl solution without and with addition of different concentrations of BBB.

C_{inh}	E_{corr}	i_{corr}	β_c	β_a	*IE*
/M	/mV	/μA cm^{-2}	/ mV dec^{-1}	/ mV dec^{-1}	/%
Blank	-499	370	112	68	-
1.7×10^{-5}	-495	148	133	73	60.0
1.0×10^{-4}	-501	52	114	69	86.1
2.0×10^{-4}	-498	39	115	71	89.5
4.1×10^{-4}	-485	31	124	66	91.5
6.8×10^{-4}	-486	21	142	86	94.5

3.3 Electrochemical impedance spectroscopy measurements (EIS)

The effect of BBB on the impedance behavior of mild steel in 0.5 M HCl solution is shown in Fig.2 (Nyquist plots).Various parameters such as charge-transfer resistance (R_{ct}), double layer capacitance (C_{dl}) were estimated in terms of the equivalent circuit of the electrical double layer (Fig.3) which was used to model the mild steel/acidic solution interface and are given in table 3. Here, *CPE* element is considered as a model of double layer capacitance (R_{ct}) like H_2O and other ion adsorbed on the surface of steel. It is apparent from these plots that the impedance response of mild steel has significantly changed after the addition of BBB in the corrosive solution. This indicates that the impedance of inhibited solution increases with increasing inhibitor concentration and consequently the

inhibition efficiency increases. The impedance diagrams acquired are not perfect semicircles and this difference has been attributed to frequency dispersion.

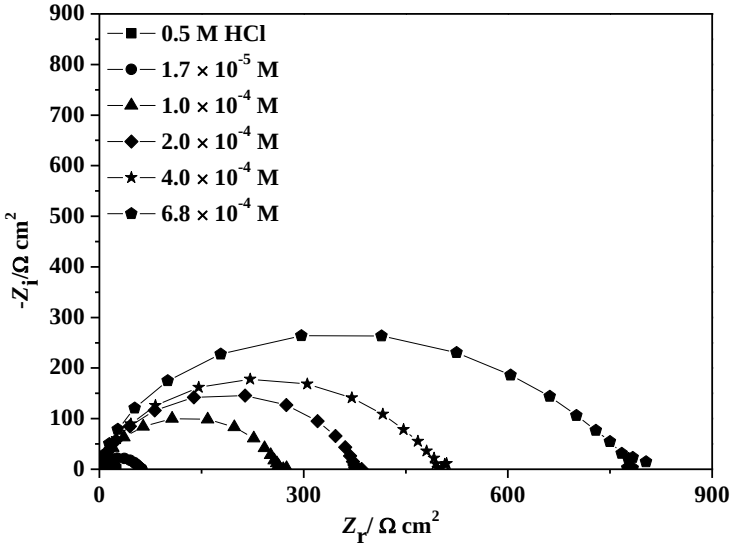

Figure 2. Nyquist plots for mild steel in 0.5 M HCl solution without and with different concentration of BBB.

C_{dl} values were calculated from the frequency at which the imaginary component of impedance was maximum ($Z_{im,\,max}$) using the following relation:

$$C_{dl} = \frac{1}{2\pi f_{max} R_{ct}} \tag{4}$$

The percentage *IE*% was calculated using the following equation and also given in table 3:

$$IE\% = \frac{R_{ct}^{0} - R_{ct}}{R_{ct}^{0}} \times 100 \tag{5}$$

Where R_{ct} and R^{0}_{ct} are charge transfer resistance without and with addition of BBB, respectively. From table 3, it is obvious that the values of R_{ct} increases and the values of C_{dl} decreased with adding BBB and this in turn leads to an increase in *IE*%. These results clearly indicate that the corrosion of mild steel in 0.5 M HCl solution is controlled by a charge transfer process [22]. The decrease of C_{dl} value suggested that the inhibition can be attributed to the decrease in local dielectric constant and/or an increase in thickness of electrical double layer which resulted from the BBB molecules adsorption at the mild steel surface/solution interface [23].

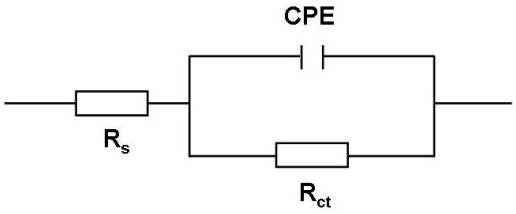

Figure 3. Equivalent circuit model used to fit the EIS results.

Table 3. Impedance parameters for the mild steel in 0.5 M HCl solution in the absence and presence of different concentrations of BBB at 303 K.

C_{inh}	R_s	C_{dl}	n	R_{ct}	IE
/M	/Ω cm^2	/μF cm^{-2}		/Ω cm^2	/%
Blank	2.81	134	0.86	21	-
1.7×10^{-5}	2.15	109	0.84	58	64.2
1.0×10^{-4}	2.22	67	0.86	262	92.1
2.0×10^{-4}	2.19	45	0.88	372	94.1
4.1×10^{-4}	2.31	23	0.89	744	97.2
6.8×10^{-4}	2.24	20	0.88	1069	98.1

The results obtained from the EIS technique in 0.5 M HCl solution were in good agreement with those obtained from weight loss method and potentiodynamic polarization method.

3.4 Adsorption isotherm

The adsorption isotherms provide basic information for the interaction between the studied inhibitor and mild steel surface.

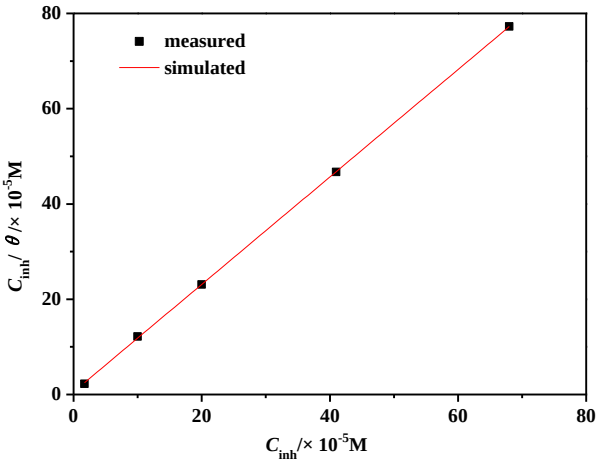

Figure 4. Langmuir adsorption plots for mild steel in 0.5 M HCl solution containing different concentration of BBB from weight loss results.

The adsorption processes of organic inhibitor on metal surface are affected by the chemical structures of organic compounds, the nature, charge and the amount of active site of metal surface, the distribution of charge in organic molecules and the type of the corrosion media. Physical and chemical adsorptions are used two types of interaction to describe the adsorption of the organic compounds. In physisorption, van der waals interaction is the main interaction between the adsorbed inhibitor molecules and metal surface. This type of interaction is of long range and weak, with adsorption free energy value in the region of -20 kJ mol^{-1}. By contrast, Chemisorption involves charge sharing and coordinate bond formation between the metal surface and inhibitor molecule [24]. The presence of a transition metal having vacant and low-energy orbital and of inhibitor with relatively loosely bound electrons or heteroatoms with lone pair of electrons is necessary for the adsorption [25]. The surface coverage values (θ) were evaluated by corrosion rate obtained from weight loss method. The (θ) values for different inhibitor concentrations were tested by fitting to various isotherms. It is found that Langmuir isotherm was the best fit isotherm (Fig.4). According to this isotherm, the surface coverage θ is related to the equilibrium adsorption constant K_{ads} and concentration of inhibitor C [26-28].

$$\theta = \frac{K_{ads} C_{inh}}{1 + K_{ads} C_{inh}} \quad (6)$$

Where C_{inh} is the inhibitor concentration, K_{ads} is equivalent constant and θ is the surface coverage. The free adsorption energy is calculated from the equilibrium adsorption constant:

$$K_{ads} = \frac{1}{55.5} \exp(-\frac{\Delta G^{o}_{ads}}{RT}) \quad (7)$$

Where 55.5 is the concentration of water in mol L^{-1}, R is the universal gas constant in J mol^{-1} K^{-1}, T is the thermodynamic temperature in K. The plot of C_{inh}/θ versus C_{inh} yields a straight line with a slope 1.12, suggesting that the adsorptions on mild steel surface followed Langmuir adsorption isotherm in 0.5 M HCl solution. The slope, equilibrium constant and regression coefficient are presented in Table 4.

Table 4. Adsorption parameters calculated from the Langmuir adsorption isotherm.

Temperature	K_{ads}	$-\Delta G^{o}_{ads}$	slope	intercept	r^2
/K	$/\times 10^5$ M^{-1}	/kJ mol^{-1}			
303	1.8	39.9	1.12	0.56	0.998

The negative ΔG^{o}_{ads} means that the adsorption of BBB molecules on the mild steel is a spontaneous process. The Values of ΔG^{o}_{ads} up to -20 kJ mol^{-1} or higher are generally consistent with physisorption. The more negative than -40 kJ mol^{-1} involves charge sharing or a transfer from the inhibitor molecules to the metal surface to form a coordinate type of bond (chemisorption) [29-31]. For the studied inhibitor BBB, the negative value of ΔG^{o}_{ads} is 39.9 kJ mol^{-1} indicates the adsorption of BBB molecules on the mild steel surface in 0.5 M HCl solution involves chemisorption and physisorption and the chemisorption is the main adsorption mode. It is concluded the adsorption of BBB molecules on the mild steel surface is owing to the coordinate bonds formed between the lone electron pairs of unprotonated N-atoms in the BBB molecule and the vacant orbital of Fe atoms which enhanced the combination tension between the BBB molecules and electrode surface [32].

3.5 AFM

The AFM technique was employed to reveal the surface microstructure of metal after corrosion test [33-36].

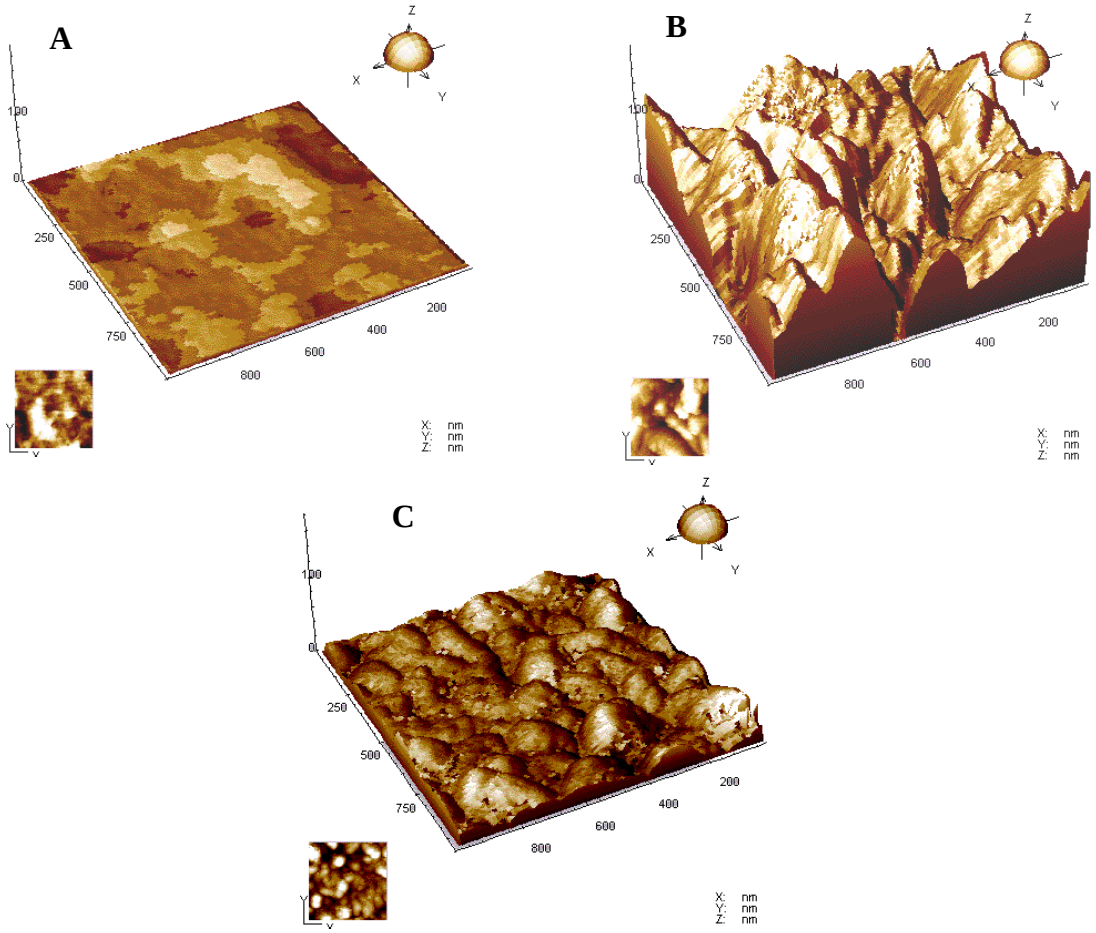

Figure 5. AFM three-dimensional images for the mild steel surface in 0.5 M HCl solution (a) before immersion, (b) 0.5 M HCl, (c) with 6.8×10^{-4} M of BBB.

Fig. 5 displayed the three-dimensional AFM image of mild steel surface immersed in 0.5 M HCl solution without and with addition of 6.8×10^{-4} M BBB for 5 h. From Fig. 5, it can be seen that the corrosion pattern of mild steel in uninhibited 0.5 M HCl solution appears uniform and some parts shows a low-mountain like structure. By contrast, the corrosion morphology of mild steel in inhibited 0.5 M HCl solution containing the inhibitor was bread-like shape, while the mild steel surface before immersion was very smooth. Through calculation, before immersion, the mean roughness is 1.11 nm (Fig. 5a). The mean roughness of the mild steel surface in uninhibited 0.5 M HCl solution is about 42.18 nm (Fig.5b) as a result of the acid attack, while in the presence of BBB, the roughness decreases to 12.69 nm of 6.8×10^{-4} M BBB (Fig. 5c) which may be a consequence of the protective film formation of an inhibitor adsorption layer, thus effectively protects mild steel from corrosion.

3.6 Quantum chemical study

Molecular modeling and frontier orbital theory might help in predicting the adsorption centre of the inhibitor molecule responsible for principal interaction with surface metal atom [37, 38, 39].

Table 5. Optimized PM_3 parameters for BBB using Hyperchem 7.5.

HOMO energy (eV mol^{-1})	-8.91
LUMO energy (eV mol^{-1})	-0.16

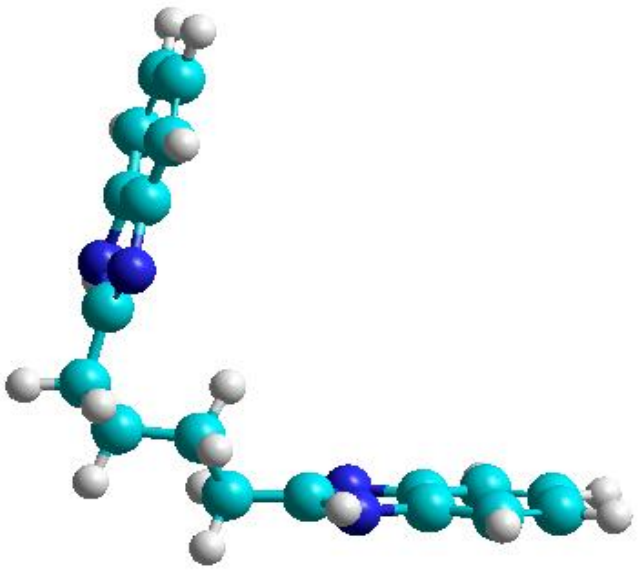

Figure 6. The optimized PM_3 structure.

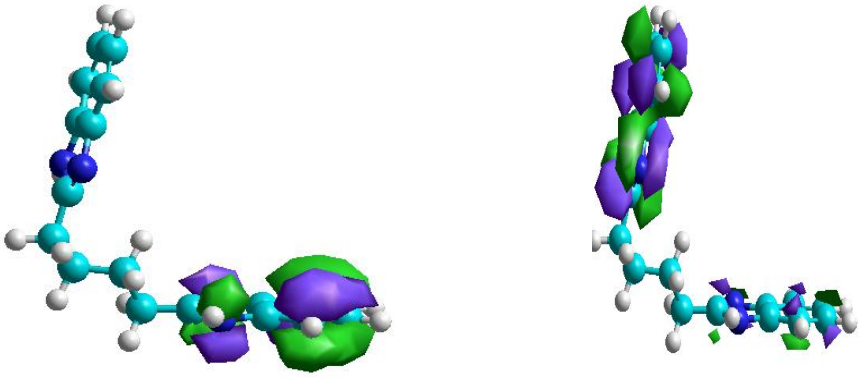

Figure 7. The frontier molecule orbital density distributions of CBO: HOMO (left); LUMO (right).

Fig.6 shows the optimized structure of the inhibitor by PM_3 method and Table 5 presents the calculated parameters of the inhibitor. The frontier molecule orbital density distributions of BBB were presented in Fig.7. As seen from the figure, the populations the HOMO focused around the benzene ring. But the LUMO densities were mainly around benzimidazole ring.

It has been proved that the higher the HOMO energy of the inhibitor, the greater the trend of offering electrons to unoccupied d-orbital of the metal; in addition, the lower the LUMO energy, the easier the acceptance of electrons from metal surface. To determine the type of interaction between iron and the inhibitor by molecular orbital approach, the energies of frontier orbitals are considered. The number of transferred electrons [40] (ΔN) was also calculated depending on the quantum chemical method.

$$\Delta N = \frac{\chi_{\mathrm{Fe}} - \chi_{\mathrm{inh}}}{2(\eta_{\mathrm{Fe}} + \eta_{\mathrm{inh}})} \qquad (8)$$

Where χ_{Fe} and χ_{inh} denote the absolute electronegativity of iron and the inhibitor molecule, respectively; η_{Fe} and η_{inh} denote the absolute hardness of iron and the inhibitor molecule, respectively. These quantities are related to electron affinity (A) and ionization potential (I).

$$\chi = (I+A)/2$$

$$\eta = (I-A)/2$$

I and A are related in turn to E_{HOMO} and E_{LUMO}.

$$I=-E_{HOMO}$$

$$A=-E_{LUMO}$$

Values of χ and η were calculated by using the values of I and A obtained from quantum chemical calculation. Using a theoretical χ value of 7 eV mol^{-1} and η value of 0 eV mol^{-1} for iron atom [41, 42]. The calculated ΔN is 0.28 which is positive. So that electrons transfer occurs from inhibitor to metal. Similar results were obtained for a group of heterocyclic diazoles as inhibitors for acidic iron corrosion [43].

4. CONCLUSIONS

(1) BBB inhibits both the anodic and cathodic processes of mild steel in 0.5 M HCl solution and inhibition efficiency enhances with the increase of BBB concentration.

(2) The weight loss and electrochemical results are in reasonably good agreement.

(3) The adsorption of BBB on mild steel surface obeys Langmuir adsorption isotherm and the chemical adsorption film formed suppresses mild steel corrosion efficiently. Electrons transfer occurs from inhibitor to iron and coordinate bond forms between the inhibitor and iron atom.

(4) Surface photographs exhibit a good coverage of BBB on mild steel.

ACKNOWLEDGEMENTS
The authors' gratefully acknowledge the financial support provided by the National Natural Science Foundation of China (Grant No. 51101106).

References

1. M. El Azhar, M. Traisnel, B. Mernari, L. Gengembre, F. Bentiss, M Lagrenée, *Appl. Surf. Sci*. 185 (2002) 197–205.
2. L. J. Berchmans, V. Sivan, S. V. K. Iyer, *Mater. Chem. Phys*. 98 (2006) 395-400.
3. F. Bentiss, M. Traisnel, L. Gengembre, M. Lagrenée, *Appl. Surf. Sci*. 161 (2000) 194–202.
4. A. B. Tadros, Abdel-Nabey, *J. Electrochem. Soc*. 138 (2) (1991) 237-242.
5. F. El-Taib Heakal, S. Haruyama, *Corros. Sci.* 20 (1980) 887-898.
6. S. A. Abd El-Maksoud, A. S. Fouda, *Mater. Chem. Phys*. 93 (2005) 84–90.
7. J. Aljourani, M. A. Golozar, K. Raeissi, *Mater. Chem. Phys*. 121 (2010) 320–325.
8. F. Bentiss, M. Traisnel, M. Lagrenée, *Corros. Sci*. 42 (2000) 127-146.
9. B. I. Ita, O. E. Offiong, *Mater. Chem. Phys*. 51 (1997) 203-210.
10. F. B. Growcok, W.W. Frenier, P. A. Andrezzi, *Corrosion* 45 (1989) 1007-1015.

11. I. Lukovits, E. Kalman, G. Palinkas, *Corrosion* 51 (1995) 201-205.
12. F. Bentiss, M. Lagrenee, M. Traisnel, B. Mernari, H. El Attari, *J. Heterocyclic Chem*. 36 (1999) 149-152.
13. F. Bentiss, M. Lagrenée, M. Traisnel, J. C. Hornez, *Corros. Sci*. 41 (1999) 789-803.
14. E. McCafferty, V. Pravdic, A. C. Zettlemoyer, *Trans. Faraday Soc*. 66 (1970) 1720-1723.
15. Y. Abboud, A. Abourriche, T. Saffaj, M. Berrada, M. Charrouf, A. Bennamara, A. Cherqaoui, D. Takky, *Appl. Surface. Sci*. 252 (2006) 8178–8184.
16. K. F. Khaled, *Electrochimica Acta* 48 (2003) 2493-2503.
17. E. S. H. El-Ashry, A. El Nemr, S. A. Essawy, S. Ragab, *Progress in Organic Coatings* 61 (2008) 11–20.
18. K. Tebbji, N. Faska, A. Tounis, H. Oudda, M. Benkaddour, B. Hammouti, *Mater. Chem. Phys*. 106 (2007) 260-267.
19. O. Olivares-Xometl, N. V. Likhanova, M. A. Dominggues-Aguilar, E. Arce, H. Dorantes, *Mater. Chem. Phys*. 110 (2008) 344-351.
20. R. Solmaz, G. Kardas, B. Yazicl, M. Erbil, *Colloids and surf., A: Physicochem. Eng. Aspects*.312 (2008) 7-17.
21. K. F. Khaled, *Electrochimca Acta* 53 (2008) 3484-3492.
22. G. Avci. *Colloids and Surfaces A: Physicochem. Eng. Aspects* 317 (2008) 730–736.
23. E. McCafferty, N. Hackerman, *J. Electrochem. Soc*.119 (1972) 146-152.
24. T. Kosec, I. Milošev, B. Pihlar, *Appl. Surf. Sci*. 253 (2007) 8863-8873.
25. A. H. Mehaute, G. Grepy, *Solid State Ionics* 9-10 (1983) 17-30.
26. M. Scendo, *Corros. Sci*. 47 (2005) 2778-2791.
27. M. Scendo, *Corros. Sci*. 49 (2007) 373-390.
28. S. L. F. A. de Costa, S. M. L. Agostinho, K. Nobe, *J. Electrochem. Soc*. 140 (1993) 3483-3488.
29. F. M. Donahue, K. Nobe, *J. Electrochem. Soc*. 112 (1965) 886-891.
30. G. Moretti, F.Guidi, G. Grion, *Corros. Sci*. 46 (2004) 387-403.
31. T. P. Zhao, G. N. Mu, *Corros. Sci*. 41 (1999) 1937-1944.
32. S. S. A. Rehim et al. *Corros.Sci*. 50 (2008) 2258-2271.
33. A. A. Gewirth, B. K. Niece, *Chem. Rev*. 97 (1997) 1129-1162.
34. I. C. Oppenherm, D. Trevor, C. E. D. Chidsey, P. L. Trevor, K. Sieradzki, *Science* 254 (1991) 687-689.
35. J. Li, D. Lampner, *Colloids Surf*. A 154 (1999) 227-237.
36. H. H. Teng, P. M. Dove, C. A. Orme, J. J. De Yoreo, *Science* 282 (1998) 724-727.
37. G. Gökhan, B. Semra, *Corros.Sci*. 52 (2010) 3304-3308.
38. G. Bereket, E. Hür, C. Öğretir, *J. Mol. Struct*. (THEOCHEM) 578 (2002) 79–88.
39. J. Fang, J. Li, *J. Mol. Struct* (Theochem).593 (2002) 179–185.
40. R. G. Pearson, *Inorg. Chem*. 27 (1988) 734-740.
41. V. S. Sastri, J.R. Perumareddi, *Corrosion* 53 (1997) 617–629.
42. M. J. S. Dewar, *J. Am. Chem. Soc*. 99 (1977) 4899–4907.
43. K. B. Samardzija, *Langmuir* 21(2005)12187-12196.

© 2012 by ESG (www.electrochemsci.org)